Strategies for controlled electronic doping of colloidal quantum dots

Alexandros Stavrinadis*, Gerasimos Konstantatos*

ICFO-Institut de Ciencies Fotoniques, Barcelona Institute of Science and Technology, 08860 Castelldefels (Barcelona), Spain

*corresponding author: alexandros.stavrinadis@icfo.es, gerasimos.konstantatos@icfo.es

Abstract

Over the last several years tremendous ~~progressed~~ progress has been made in incorporating Colloidal Quantum Dots (CQDs) as photoactive components in optoelectronic devices. A significant part of that progress is associated with significant advancements ~~made in achievingon~~ controlled electronic doping of the CQDs and thus improving the electronic properties of CQDs solids. Today, a variety of strategies exists towards that purpose and this minireview aims at surveying major published works in this subject. Additional attention is given to the many challenges associated with the task of doping CQDs as well as to the optoelectronic functionalities and applications being realized when successfully achieving light and heavy electronic doping of CQDs.

1. Introduction

The research in Colloidal Quantum Dots (CQDs) has progressed tremendously over the last 30 years leading to substantial advances related to making these materials, understanding and controlling their physicochemical properties and utilizing them in every-day applications [1]. The most admired property of these semiconducting particles is the dependence of their color on their size due to the well-known quantum confinement effect[2]. This property has naturally directed great efforts in using CQDs as photoactive components in various optoelectronic applications like solar cells[3,4], photodetectors[5,6], light emitting diodes[7,8] where spectral selectivity is a powerful leverage for high performance and disruptive functionalities. The advances in these applications have been substantial: over just 15 years of research the power conversion efficiency of CQD based solar cells has risen from <2%[9,10] towards approaching 10% [3,4], CQD based photodetectors have outperformed state of the art single crystal InGaAs ones[5] and CQD based LEDs (QLEDS) displays have been integrated in flexible and wearable electronics[11]. Such advancements would not have been possible without the significant

progress in controlling not only the *optical* but also the *electronic* properties of these *optoelectronic* materials.

Electronic doping of CQDs can lead to several technological improvements and breakthroughs. One example is the realization of CQD mid-IR photodetectors that rely on intra-band optical photoexcitations instead of the inter-band ones which are currently utilized in most CQD applications[12]. Intra-band transitions become technologically relevant upon stable and permanent doping of a CQD film in which carriers in equilibrium are located in the first excited state (1Se), that would have otherwise been empty. Such a possibility could lead to disruptive technologies in mid-IR CQD optoelectronics competitive to the existing high-cost ones based on HgCdTe, GaAs/AlGaAs quantum well infrared detectors and quantum cascade lasers[12–14]. Doping has also been suggested to be important for lasing ~~in CQDs~~ through inter-band transitions as it can result in a 10-fold decrease of the optical pump threshold required for achieving the lasing effect[15,16]. In more conventional applications like solar cells, precise electronic doping of CQDs is needed in optimization of p-n junctions [17,18] and the fabrication of p-n and graded doping CQD homojunctions for high charge collection efficiencies[17–21]. To summarize, advancing CQD optoelectronics depends dramatically on achieving control over their electronic doping, similar to the case of traditional single crystalline semiconductor technology.

In bulk semiconductors the process of changing the electrical properties of a certain compound semiconductor without altering significantly its crystal phase/structure is described as “doping” and refers to controlling the density and nature of minute quantities of electrically active crystal impurities in the material. These impurities can act as free electron donors, acceptors or traps and thus their presence and degree of ionization determine the Fermi level of the host semiconductor and therefore its carrier density and conductivity. In addition, carrier mobility is also affected by doping since mobile carriers can be scattered by charged impurities, can be trapped (and de-trapped) by shallow-trap states or even directly hop amongst neighboring trap sites if these are spatially and energetically close. Trap sites also mediate additional radiative and non-radiative carrier recombination pathways resulting to loss of mobile carriers. It is thus clear that in general the structural impurities or dopants of a semiconductor crystal affect crucially its electronic properties. Some of the most relevant types of electronically active crystal impurities are atomic vacancies and other associated point crystal defects, interstitial and substitutional atomic impurities, dangling bonds, chemical impurity species on the surface of the crystals or combinations of the above.

It is thus evident that doping CQD can be a much more involving task in view of their very high surface to volume ratio. The abundant surface of CQDs is naturally a source of impurities, dangling bonds and off-stoichiometric domains that have been responsible for the low carrier mobilities, poor quantum yield and formation of shallow donor or acceptor sites and deep electronic trap states that inadvertently lead to electronic doping in a non-controlled manner.[22–24]

2. Challenges in doping CQDs.

A single CQD consists of a few hundreds to thousands of atoms with a large number of them located on its surface[2]. The surface of CQDs is the first main source of impurities that needs to be controlled for accurate electronic doping of a single dot as well as of CQD films (or solids in general) composed of closely packed dots[25,26]. Atoms on the surface facets of the dots may exhibit dangling bonds that introduce mid-gap trap states[27–29]. In reality, rarely do these bonds remain dangling; instead they are passivated by organic or inorganic molecular and atomic ligands which intentionally or not are introduced or adsorbed by the environment. Fatty acids and amines are typical examples of long organic molecules that are purposely used to passivate the dots´ surface and provide stability in non-polar organic solvents[30]. Oxygen[31,32] or hydroxyl[33] moieties on the other hand are typical examples of often unintended yet present surface ligands. Ligands are important doping factors not only because they passivate dangling bonds and balance a possible excess charge the CQDs[29,34], but also because they may act as electron donors[35] or introduce electronic trap states[29].

The surface of the dots can cause an additional doping impurity mechanism, due to the stoichiometry deviation from the bulk. In binary, ternary etc. semiconductors like lead and cadmium chalcogenides deviation from their ideal anion to cation stoichiometry ratio can be a source of doping since cations are considered as electron donors and anions are considered as electron acceptors[28,36,37]. In addition, excess cations or anions in CQDs and their resulting dangling bonds may induce trap states close to conduction or valence bands respectively[27]. In reality, CQDs are typically non-stoichiometric and the aforementioned chalcogenides are typically cation rich with the excess cations forming a cell of the surface of the dots[32,38–44]. This effect depends on the size and thus surface-to-volume ratio of the dots, but also on the synthetic method followed as well as on the post-synthetic treatment of them towards CQD solid formation. Stoichiometric deviations of the CQDs can also take place in the presence of crystal

defects like atomic vacancies[45–48] or formation of cation dimers[38] on the surface of the dots that may serve as additional sources of charge imbalance and trap state formation.

The stoichiometry of the dots as a doping factor is taken into account in the charge orbital balance model that has been proposed to predict the doping character of single CQDs, and has being successfully coupled with experimental findings for PbS CQDs[34]. That model relies on summing all positive and negative ionic contributions of all cationic and anionic species forming the dots, including surface ligands[34]. The valence state of each ionic component of a CQD is an obvious parameter to be considered when predicting its net doping character and that is particularly important for predicting the relative effect of aliovalent doping impurities, the use of which is of course trivial in bulk semiconductor technology. Doping CQDs however with aliovalent impurities comes with additional challenges that are discussed in the following.

Several decades ago Turnbull proposed that very small crystals will tend to contain fewer defects[16,49,50] compared to large ones. The concept of self-purification has been studied for CQDs and has been proposed as a mechanism to account for the difficulties met in incorporating dopants in CQDs for certain systems such as doping CdSe CQDs with manganese[16,50–52]. In addition heavy doping of a CQD with elemental impurities may destabilize its electronic and crystal structure[53] and inhibit its growth[54]. A second major practical challenge is to achieve homogenous doping across an ensemble of CQDs. In a process of doping a batch of CQDs, the doping density will vary from dot to dot according to a Poisson distribution[54,55] and for electronic applications this is a non-ideal case since doping inhomogeneity will translate to optoelectronic inhomogeneity. The latter can also arise from differences in the spatial distribution of dopants within individual dots; for example it has been demonstrated that dopants have different optoelectronic effects when located within the core of the dots as compared to being on the surface of the dots[56]. Thus doping CQDs with charged impurities also requires control over the incorporation and position of the dopants in the CQDs.

Another consequence of the high surface to volume ratio of the CQDs and the limited number of available energy states at the band edge of a single CQD is that the latter can be heavily doped by remote charge transfer from other molecules[57–59], nanocrystals[60,61] and electron transfer media[62,63] located at the vicinity on the CQDs surface. Remote doping of CQDs has received significant attention as a means to studying the optoelectronic effects upon heavy charging of the CQDs without altering their structure as well as due to its relevance in advanced device architectures like bulk heterojunctions solar cells of CQDs with other nanomaterials.

Nevertheless, heavy charging of CQDs may initiate charge compensation processes: for example the ability of certain CQD materials to be negatively charged by excess of electrons in the conduction band may be limited by transfer of the excess free electrons to the surface of the dots and their consumption there in permanent electrochemical reactions[16,58,64]. Such an effect will depend on the electron energy determined by both the CQD material and the degree of quantum confinement and can explain why certain materials like nanocrystalline ZnO can maintain electrons in their conduction band for longer time periods compared to others like CdSe CQDs[16].

Electronic doping control of CQDs can thus be achieved through several methods and this review is focused on describing major CQD doping schemes categorized as: i) doping via oxidation, ii) doping via ligand control, iii) doping via stoichiometry and defects iv) doping via aliovalent impurities, v) remote doping. We further emphasize to reports and materials related to two major applications: photovoltaics and photodetectors. We deem useful to focus on works related to doping CQD materials which are photoactive in the visible and NIR parts of the spectrum and with demonstrated impact of the doping process on their electronic properties. Not surprisingly, the majority of these works concern two of the most heavily researched CQD material families: cadmium and lead chalcogenides.

3. Doping schemes

3.1 Doping via oxidation

As-synthesized CQDs are passivated by long ligands that inhibit oxidation of their surface. Upon fabrication however of CQD thin films for electronic devices, the original long ligands are usually replaced by shorter ones in order to promote inter-dot electronic coupling and this process renders the CQD surface vulnerable to oxidation[31,32,65]. In agreement to the charge orbital balance model for predicting the doping character of CQDs, oxygen anions act as p-type dopants when reacting with the surface of metal chalcogenide dots as has been repeatedly confirmed for PbS and PbSe and CQDs [32,35,66]. Oxidation of the dots leads to p-type doping with shift of the Fermi level towards the valence band and the formation of electron trap states due to lead oxide and sulfate species formed on the surface of the dots. For the case of PbS CQDs, Konstantatos et al. have identified three trap levels at 0.1, 0.2 and 0.34 eV below the conduction band and each trap was further assigned to a specific oxide species: $PbSO_3$, $PbSO_4$

and lead carboxylate respectively[67]. This material-energy mapping allowed for surface engineering towards avoiding the deepest traps and thus improving the temporal response of PbS photoconductors under illumination[67]. The extent and nature of oxidation in CQD films can be partially controlled by the ligands used for passivating the surface of the dots[67] and by the size of the CQDs[32]. Tang et al. reported that ~~the electrical characteristics of~~ solar cells based on thin films of 1,2-ethanedithiol (EDT) passivated PbS CQDs having an exciton peak in the 900-100 nm range were much more stable compared to larger PbS CQDs[32]. The stability of the smaller CQDs was ascribed to their rich (111) and (220) facet termination as compared to the (200) facets of larger dots[32], as the latter are more prone to oxidation via the formation of sulfates. Although oxidation of PbS CQDs is generally undesired when aiming for n-type or intrinsic films, it is ~~also~~ useful and purposely induced when heavily ~~requiring heavily~~p- doped ~~p-type~~ films ~~i.e.~~ as part of p-n homojunction PbS CQD solar cells are needed[20].

Oxygen may not only act as a p-dopant when reacting with the lead chalcogenide CQDs but also when it is just physically adsorbed -in its molecular form- on the surface of the CQDs[68]. Leschkies et al. studied the effect of oxygen and nitrogen gas exposure on the electrical characteristics of EDT passivated PbSe CQD FETs [68]. They found that O_2 gas is a p-type dopant, and as long as the O_2 pressure was maintained below a certain level (10^8 langmuir) this doping effect was reversible upon removal of the O_2 atmosphere[68]. They argued that at low exposure levels the O_2 is adsorbed physically on the CQDs creating electron acceptor states while the O-O bond remained intact. However, at higher exposure levels (10^{10} langmuir) the oxygen induced irreversible changes on the electrical properties of the PbSe QD films, likely due to dissociation of the O-O bond and permanent oxidation of the CQDs[68]. On the other hand N_2 gas exposure was found to promote n-doping of the CQDs, with the effect being reversible upon removal of the nitrogen atmosphere[68]. These observations can be explained by considering that nitrogen passivates about 0.6 electron traps per quantum dot which corresponds to about 0.01% N_2 surface coverage[68]. We note, that the reversible to some extent effect of oxygen on the conductivity character of lead chalcogenide quantum dots may at least partially explain why the Fermi level of PbS CQDs films as measured with Ultraviolet Photoelectron spectroscopy[69] under high vacuum appears to be closer towards the conduction band as compared to when is measured with other techniques like kelvin probe measurements[70] performed under ambient atmosphere conditions[21].

3.2 Doping via ligand control

As synthesized CQDs like CdSe and PbS are usually cation rich with the excess metal atoms located on their surface[32,38–44]. Thus although the metal rich character can be lowered by tailoring the ligands used during the growth of the dots and size of the dots, as synthesized CQDs are generally passivated by anionic ligands which balance the excess negative charge of the dots. When fabricating CQD films for optoelectronics, ligands are further chosen to be short as to promote inter-dot electronic coupling and thus ~~charge~~ improve conductivity[35,66,71–73].

In CQD thin films, judicious choice of the ligands and their functional group(s) attached on the CQD surface has a significant impact on the doping characteristics of the films. One of the first and most dramatic demonstrations of doping CQDs through ligand attachment has been reported for PbSe CQD films treated with hydrazine[35]. Hydrazine treatment in an inert atmosphere can switch the conductivity of the film from p-type to n-type[35]. Upon desorption of the hydrazine from the film or exposure to an oxygen atmosphere the conductivity switched back to p-type, an effect which is further reversible by subsequent hydrazine treatment[35]. That indicates that hydrazine promotes n-type conductivity by donating electrons and chemically reducing the surface of the CQDs. Other, conventional for optoelectronic applications, ligands may also impact doping in CQD thin films. For example, in lead chalcogenide CQD films the use of short thiols, amines and acids as ligands impacts the oxidation rate and oxide species formed on the surface of the dots which as discussed act as p-type dopants[67]. Small dithiols in particular EDT and 1, 3-benzenedithiol (BDT) are commonly used for the fabrication of PbS and PbSe CQD solar cells because they lead to enhanced surface trap passivation of the dots and thus increased open circuit voltage of the cells[66,71–73]. The mobility-carrier lifetime product of PbS CQDs ~~and solar performance~~ can be further increased ~~when choosing~~by using 3-mercaptopropionic acid (MPA) ~~instead~~ as ~~the~~ a ligand which compared to dithiols results to ~~enhanced~~ better passivation of mid-gap trap states ~~acting recombination centers~~[74]. Mid-gap trap states on such CQD films however may also be formed by organic and inorganic byproducts induced by the ligand exchange process such as metallic Pb (also described as “under-charged” Pb)[75] and high molecular weight complexes of lead oleate with small conductive ligands[76]. Identifying and eliminating such electronically active species is beneficial for doping control.

Surface passivation with atomic ligands such as halides (I^-, Br^-, Cl^-) has also been reported to have significant impact on the doping character and mobility characteristics of lead chalcogenide CQD films rendering them n-type; this concept is described in a series of works

published by the Sargent group at the University of Toronto[20,77–80]. In that doping scheme, the n-type of the dots is assumed to result from passivation of surface trap states, prevention of oxidation by the halide ligands and possibly due to substitution of S^{2-} with the monovalent halide anion close to the surface of the CQDs as schematically shown in Figure 1a[80]. The electronic properties of the CQD films incl. their charge carrier mobility and concentration depend on the halide element and concentration as shown in Figures 1b,c[80]. Prior reports on this method demonstrated the unstable n-type character of the halide treated films due to oxidation when exposed to ambient atmosphere[34,80]. In that case halide incorporation was achieved via ligand exchange during CQD film deposition using organic salts dissolved in polar protic solvents. The instability/oxidation drawback drove research towards further optimization of the halide passivation strategy by adding a post-synthetic halide treatment of the dots in solution prior to the subsequent halide treatment of the dots in solids during CQD film formation[77]. It was found that the post-synthetic halide treatment in solution resulted to passivation of surface sites that could not be passivated during film deposition[77]. In fact the polar protic solvents used typically during film deposition may cause desorption of Cl^- and Br^-, while I^- was much more robust[77]. Overall, the scientific progress in this subject has resulted to methods for fabricating halide passivated air-stable n-type PbS CQDs films for solar cells.

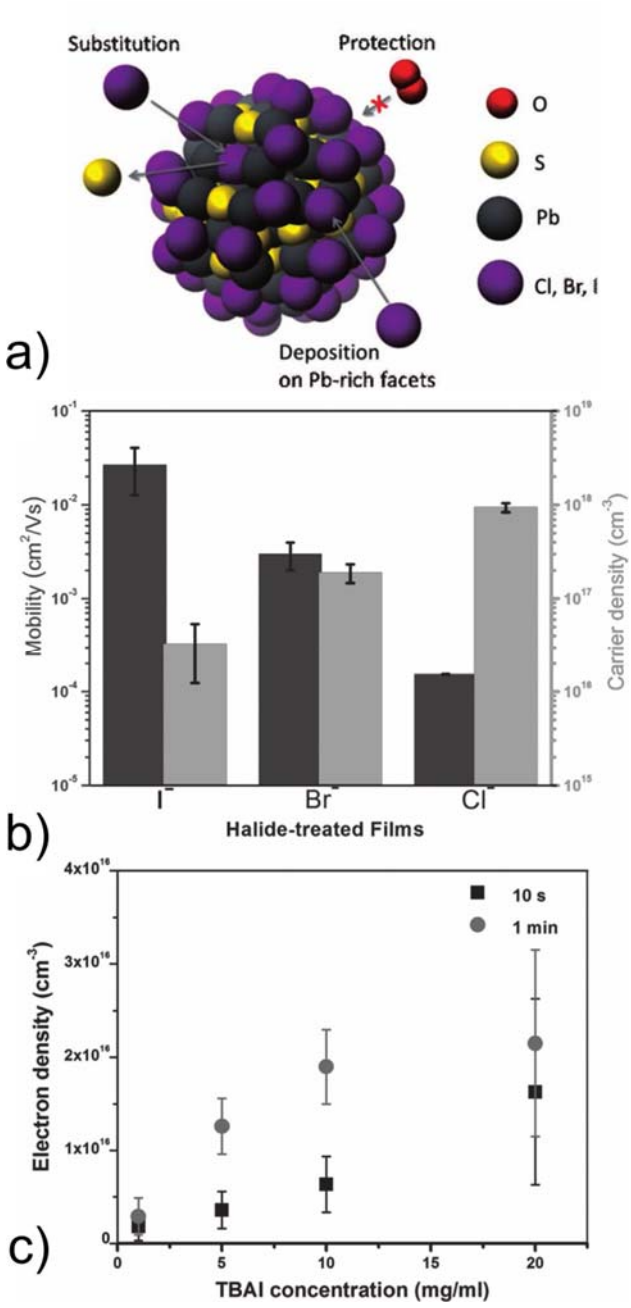

Figure 1. a) Schematic illustration of passivation of the surface of PbS CQDs with halide ions and related mechanisms for promoting n-doping. b) Electrical properties of PbS CQDs for different halide ligands as extracted by FET measurements. Grey colour refers to carrier density and black to mobility values. c) Electron density as a function of halide treatment experimental parameters. Adapted with permission from ref. [80], Copyright 2012 WILEY-VCH Verlag GmbH & Co.

The doping character of CQD films can be further controlled by combining organic and inorganic ligands. Ip et al. described that a hybrid ligand passivation (CdCl+ EDT or MPA) is superior compared to either simple halide or organic passivation[79]. The reason is that the hybrid

passivation gives a surface Pb/ ligand ratio of almost unity meaning that the surface charge of the dots´ Pb-rich core is nearly balanced by the surface ligands suppressing thus trap state density, which for the PbS films was found to be about 10^{17} cm^{-3} from transient photovoltage and thermal admittance spectroscopy measurements[79]. Organic ligands alone cannot fully passivate all surface sites because the surface coverage by the ligands is sterically hindered[81]. A judicious choice of ligands whose bulkiness determine the surface coverage on the CQD surface and thereby passivation and doping allowed for the fabrication of graded doping depleted heterojunctions that benefited from additional charge separation in an engineered p^+/ p CQD interface[81].

Halide anions are not the only inorganic ligands being investigated for CQD doping control, some other notable ligands are thioacyanate[82], chalcogen ions and metal chalcogenide complexes[83,84]. Passivation of the CQD surface with anionic ligands results to a negatively charge surface layer of the CQDs[85,86], which may further results to the dots´ mutual repulsion and stability in polar solvents[84]. The negative surface charge can be counterbalanced by the use of cations in the solvating medium and that concept has been used by Nag et al. who studied the effect of metal cations on the optical, electronic, magnetic and photocatalytic properties of CQDs[84]. In their study the cations were not introduced inside the CQDs but in between the dots[84]. It was shown that metal cations such as Cd^{2+}, Ca^{2+}, In^{3+} may bind to S^{2-} passivated CdSe and InAs CQDs[84]. Due to their S^{2-} passivated surface, the CQDs presented a negative surface charge and the subsequent addition of cations further inverted that charge from negative to positive and enhanced the PL of the quantum dots due to a decrease in the density of surface trap states [84]. The inter-dot distance varied significantly with the metal cation used, for example for CdSe/S^{2-} CQDs that distance was reduced from 1nm for the case of K^+ to almost zero for Cd^{2+} and In^{3+}. That impacted significantly the electronic properties of the CQD films as studied with FETs[84]. The drain-source current and mobility of the CQD films exhibited a 100-fold increase when switching from K^+ to Cd^{2+} and In^{3+} passivation, and an accompanying n-type doping effect as observed[84]. Nag et al. described that the metal cation used determines the majority carrier type and density in a manner similar to substitutional doping in bulk semiconductors i.e. the monovalent K^+ promotes p-doping while the trivalent In^{3+} provides n-doping. In another example, the conductivity of nanocrystalline CdTe/Te^{2+}/K^+ FETs switched from ambipolar p-type to n-type when In^{3+} replaced K^+ [84]. The doping method described by Nag et al. is more akin to the remote doping scheme where the ionized impurities are not integrated in the nanoparticles´ crystal structure[84,87].

The choice of either organic or inorganic ligands used for the passivation of the CQDs will also affect their surface electrostatic dipole and thus the energy of all electronic states with respect to vacuum zero energy. That was demonstrated recently for a variety of organic and inorganic ligands in PbS and PbSe CQDs films for solar cells[69,88]. This concept has been used for optimizing band level engineering and performance of multilayer CQD solar cells with power conversion efficiencies exceeding 8.5% [89]. Furthermore, such a dipole effect has been proposed as the underlying reason for the recent discovery of air stable n-type heavy doping of HgS and HgTe CQDs by the Guyot-Sionnest research group at the University of Chicago [12,90]. As reported by Jeong et al. the air stable n-doped HgS CQDs have a bandgap in the NIR (around 0.6eV) and exhibit many novel properties: intra-band absorption and PL in the mid-IR and transfer of oscillator strength in between the intra-band and inter-band transitions[90]. These properties, as shown in Figure 2a, are controlled by the successive treatment of the surface of the CQDs with Hg^{2+} or S^{2-}, with the first inducing heavy n-doping and the second removing the doping effect. In addition, it was confirmed that the doping effect is due to charging of the 1Se state with electrons[90]. As illustrated in Figure 2b the dependence of the doping on the surface ion treatment was attributed to the impact successive ion treatments have on the CQDs´ surface electrical dipoles and thus on the dots energy level position with respect to the Fermi level which is determined by the dots´ external environment[90]. These very important findings paved the way for the realization of CQD intra-band photodetectors[12] which will be further presented towards the end of this review.

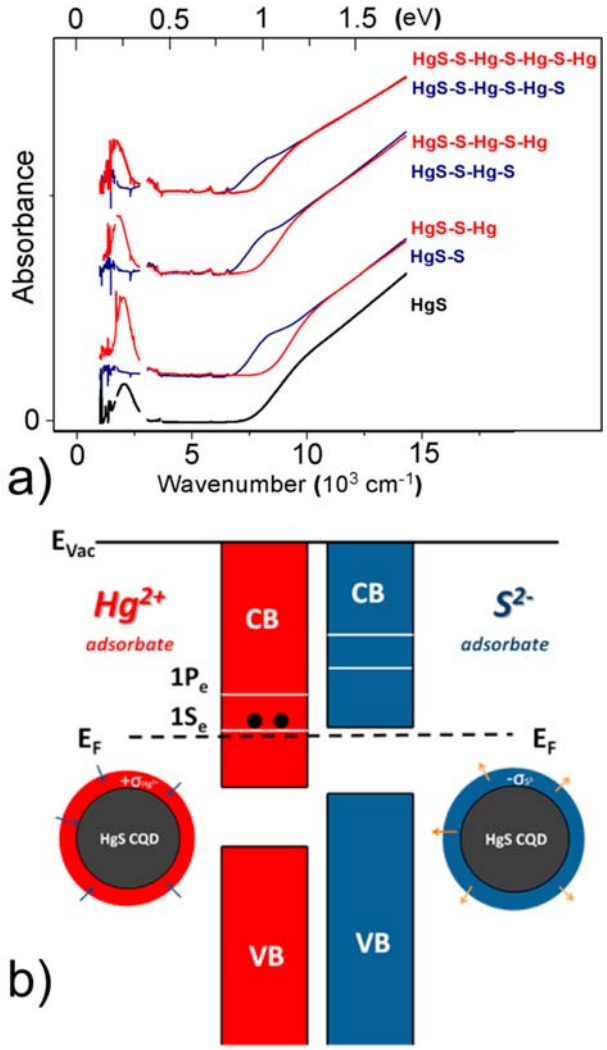

Figure 2. a) Optical absorption spectra of HgS CQDs treated successively with Hg^{2+} and S^{2-}. The spectra show transfer of oscillatory strength between the dots´ inter-band transition (at about 0.75-1eV) and the intra-band 1Se-1Pe transition at about 0.25eV, due to charging and de-charging of the 1Se states with electrons upon Hg^{2-} and S^{2-} treatment respectively. b) Schematic illustration showing that the charging/de-charging effect of the CQDs is attributed to an electrostatically induced shift of the VB and CB states with respect to Fermi level, depending on the surface adsorbate. Adapted with permission from ref. [90], Copyright 2014 American Chemical Society.

3.2. Doping via stoichiometry and defects

The stoichiometry of binary ternary etc. CQDs can impact significantly their doping character since it is directly related to the cation/anion ratio as well as the presence of structural defects such as vacancies and dangling bonds and their related trap states[36,37,91]. For example Cu_2S is known to be prone to formation of copper vacancies, a process which is accelerated upon

exposure to air, and this effect leads to degenerate electronic doping and the appearance of a plasmonic peak in the optical absorption spectrum of Cu_2S nanoparticles[46,47]. Bekenstein et al. illustrated that is possible to achieve controlled p-type doping of Cu_2S nanoparticle films by annealing them at relatively low temperatures (<400K) in an inert atmosphere[91]. That process induced the formation of copper vacancies due to diffusion of copper atoms to the surface of the nanocrystals and the nanocrystalline nature of the material further promotes that effect[91]. That doping method resulted to an increase of the films´ conductivity by up to 6 orders of magnitudes and an increase of hole concentration by more than four orders of magnitude[91]. Increase of conductivity and p-type doping was also observed at a single particle level using C-AFM and STM. It was observed that the annealing led to a shift of the E_F towards the valence band and appearance of mid-gap states[91].

In another report, the direct impact of cation/anion stoichiometry on the doping character of CQD films was shown by Oh et al.[36] Thermal evaporation of excess Pb or Se on top of films of PbSe (or PbS) CQDs could render them p- or n-type respectively[36]. The majority carrier concentration changed from 10^{16} cm^{-3} for reference films to 10^{19} cm^{-3} for Pb-infused PbSe films and 10^{18} cm^{-3} for Se infused films, as studied by measuring FETs[36]. The electrical characteristics could be precisely controlled and optimized by the amount of Pb and Se evaporated on the films, and carrier mobility values were improved from 0.02 $cm^2V^{-1}s^{-1}$ for reference films to record values of 10 $cm^2V^{-1}s^{-1}$ for doped films. Also, at large excess of Pb or Se the films behaved as semi-metallic due to degenerate doping[36]. It must be mentioned that the efficiency of the doping process was reported to be low: the addition of 33 Pb atoms per CQD resulted to just 0.5 added electrons per dot, similarly only 0.3 extra holes resulted from the addition of 47 atoms of Se per CQD[36]. The low doping efficiency was attributed to the following factors: 1) not all of the vacuum-deposited atoms were bound to the CQDs 2) not all added atoms were sufficiently ionized 3) some dopants were compensated by unintentional doping species like oxygen and defects[36]. Despite this reported limitation, the work by Oh et al.[36] demonstrated a promising route towards precise electronic doping control and optimization of CQD films for various optoelectronic applications.

3.4. Doping via aliovalent impurities

Aliovalent (heterovalent) impurity doping is the most standard method for doping bulk semiconductors. Despite the many challenges we discussed earlier related to doping CQDs with elemental impurities, extensive progress has been made on the subject of electrically active doping impurities in CQDs. This topic that has benefited greatly by other closely related subjects like the study of cation exchange reactions on colloidal nanoparticles for material transformation[92,93], doping CQDs with optically or magnetically active impurities[56,94–96], electrically active doping of high bandgap oxide nanoparticles[97] and of nanoparticles like Si nanocrystals[98–101] synthesized via non-solution based methods. This section of the review however is focused on electrically active doping impurities of CQDs having an energy of bandgap in the visible and IR and synthesized via solution-based colloidal chemistry.

Several works exist on doping CdSe CQDs with trivalent cations of Ga[64], Al[102], In[102–106] which should act as electron donors upon replacing Cd^{2+} . Wills et al doped CdSe in solution with Al and In [102] . The two dopants were introduced in solution after nucleation of the dots, and their addition was followed by further growth of a CdSe cell. They found that half of Al remained on the surface of the CQD while half other was uniformly distributed in the core[102]. For In however they found that it mostly lied at the radial position at which it was added during the overall growth procedure[102]. That finding indicated that indium does not easily diffuse through the CdSe lattice, in agreement with similar works on this material system[104,105] . For the case of Al-doping, thin film transistor measurements confirmed that it promotes n-type doping of the CQDs, and raises the Fermi level and carrier mobility values from 0.2 to 0.9 $cm^2V^{-1}s^{-1}$ [102]. Ga-doping has also been shown to raise the Fermi level of CdSe CQDs and increase n-type conductivity as well as to enhance the chemical reactivity of the dots due the dopant's electron donating character[64]. Regarding In-doping in CdSe CQDs, Choi et al. reported remarkable n-doping effects when introducing the impurities in CQD films by thermally induced infusion of In that was priory evaporated atop the films[103]. In that work doping with In was found to cause a shift the E_F towards the conduction band edge of the CQD films and result to increase of the electron mobility of the films as studied via electrical characterization of FETs[103].

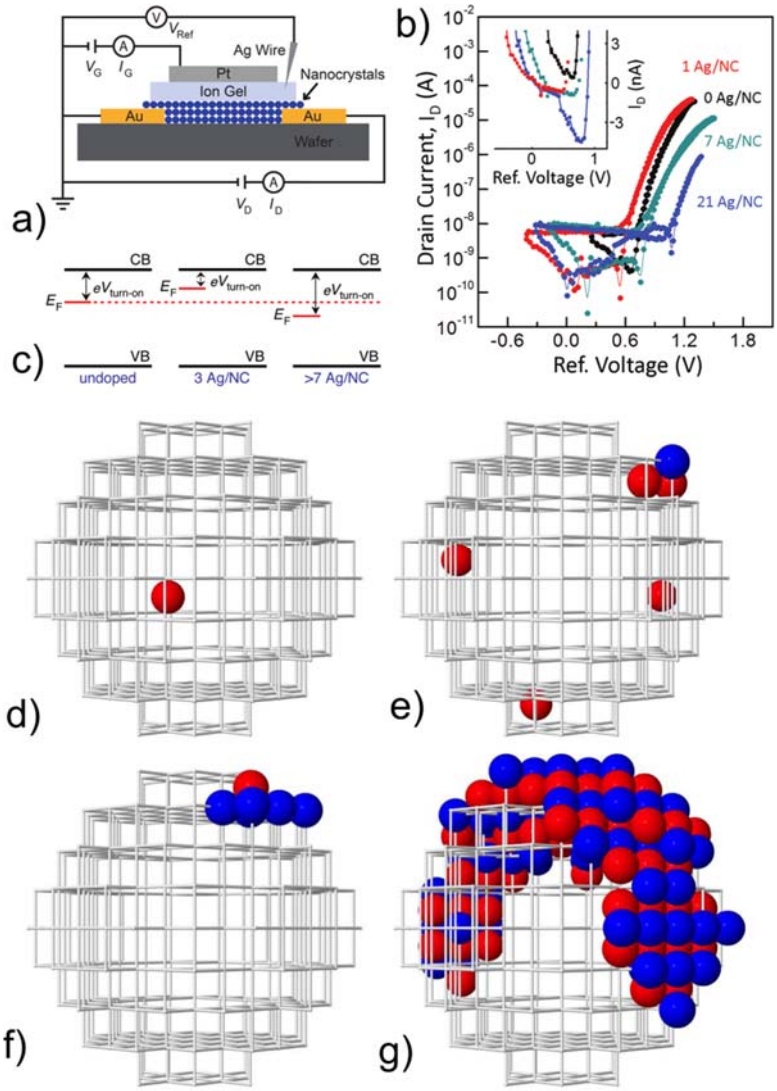

Figure 3. a) Thin film transistor device architecture used to measure electrical properties of Ag-doped CdSe CQDs films. b) Drain-current Vs Reference voltage characteristics from TFTs for different doping levels for monitoring doping trend as a function of different Ag-doping levels per CdSe nanocrystal (NC). C) Schematic describing that at low concentrations Ag acts as n-dopant and at higher ones as p-dopant. N-doping is achieved if Ag^{2+} is an interstitial impurity and p-doping if Ag substitutes Cd^{2+}. This explanation is corroborated by computational simulations of the cation-exchange reaction leading to doping of the NCs (CQDs) showing that d) a single Ag^{1+} per NC moves through interstitial (red ball) sites and e) as more Ag^{1+} are added substitutional incorporation occurs, and as reaction proceeds f) substitutional incorporation dominates with progressive formation of g) a separate Ag_2Se phase. Figures a,b,c adapted with permission from ref. [107], Copyright 2012 American Chemical Society. Figures d,e,f,g adapted with permission from ref. [108], Copyright 2014 American Physical Society.

CdSe CQDs have also been doped with monovalent metal cations like Ag^{1+} [107]and Cu^{1+} [109] which should act as electron acceptors when replacing Cd^{2+}. Overall, these efforts have not resulted yet to the formation of p-type CdSe CQDs. Doping with Cu^{1+} was reported to introduce

changes in the density of states of Se, and result to charge imbalance in the dots and appearance of trap states due to the formation of vacancies [109]. Doping with silver ions has been achieved by the Norris group and several interesting findings associated with these doped CQDs were reported: Sahu et al. [107] studied post-synthetic doping of CdSe with Ag^{1+} via cation exchange reactions purposely slowed down as to achieve controlled addition of few dopants per CQD. They found that at dopant concentrations up to 2 Ag^{1+} per CQD the PL of the dots increased and at higher concentrations the PL decreased again. To account for these optical effects they proposed that at low doping concentrations silver ions were located in interstitial lattice sites acting as electron donors (n-doping) and at higher concentrations the dopants were substituting Cd^{2+} acting as electron acceptors (p-doping) [107]. Having in mind this model, the initial increase in the PL could be explained considering that the extra electron from the interstitial Ag^{2+}, would leave the impurity and be trapped on the surface of the CQD leaving the impurity positively charged[107]. The presence of positively charged impurities could explain the increased PL in accordance with other works describing such an effect for CQDs[110,111]. While the increase of the PL upon the introduction of an electron donating dopant is counterintuitive due to enhanced Auger recombination[112], the doping model proposed by Sahu et al. [107] was supported with a plethora of further experimental evidence. They fabricated and tested CQD TFTs, as schematically described in Figure 3a, and measurements confirmed the non-monotonic doping character with increasing impurity concentration[107]. The position of the turn-on voltage in current-voltage characteristics of the TFTs as shown in Figure 3b indicated that with increasing Ag content, E_F first shifts towards the conduction band edge as described in Figure 3c and further shifts the other way as the doping content is increased[107]. In a later paper, Ott et all [108] using DFT and kinetic Monte Carlo simulations confirmed that Ag diffuses in CdSe through interstitial sites and a single Ag impurity is likely to stay as an interstitial impurity and act as electron donor. However, as more silver ions are introduced in the CQD and the reaction proceeds in time, a single Ag^{1+} is more likely to knock out and substitute a Cd^{2+} further triggering similar events and accelerate the cation/exchange reaction towards complete transformation of CdSe to Ag_2Se [108]. Time-frames of such a simulated reaction at a single dot level are shown in Figures 3d-g [108]. More recently reported EXAFS studies confirmed that Ag ions are located inside the CdSe CQDs occupying interstitial sites for doping concentrations below 2.5% [113].

InAs CQDs have also been doped with aliovalent cations like Cd^{2+} [114], Cu^{+}, Au^{3+} and Ag^{+} [53,115]. Geyer et al. [114] reported that the conductivity of InAs nanocrystal solids changed from n-type

to p-type upon doping the nanocrystals with cadmium. The original n-type behavior was observed for InAs nanocrystals films treated with thiols which are known to passivate surface trap states of InAs nanostructures [114116]. However the nanocrystal films exchibited p-type conductivity when the nanocrystals were doped with cadmium by refluxing the original particles in cadmium[114]. Geyer et al. further described two possible mechanisms that may be responsible for the observed change of conductivity upon doping: 1) substitution of In^{3+} by Cd^{2+} and the formation of acceptor states near the valence band, 2) surface attachment of cadmium on the NCs and formation of acceptor states near the valence band[114]. In another work, Mocatta et al studied post-synthetic doping of InAs QDs with Au^{3+}, Ag^{+}, Cu^{+} [53]. They found that all three dopants could enter the QD structure and cause different doping effects. Ag^{+} doped the CQDs by substituting In^{3+}. The p-type doping was evident by STM (scanning tunneling microscopy) measurements revealing a shift of E_F towards the valence band[53]. Doping with Ag^{+} was further accompanied by the formation of energy states close to the valence band of the CQDs[53]. The differences between STM spectra of single InAs CQDs doped with different cations can be observed in Figure 4[53]. Doping with silver also caused the appearance of an Urbach tail and a red shift on the exciton absorption peak[53]. On the other hand, Cu^{+} behaved as an interstitial impurity causing n-type doping also evident by STM measurements and an observed blue shift of the exciton optical absorption peak presumably due to the Moss Burstein effect[53]. Mocatta et al further noted that the formation of dopant states close to the valence or conduction bands of the CQDs may explain the absence of bleaching of their first exciton absorption peak despite the heavy elemental doping densities applied[53]. Finally the researchers reported that Au^{3+} doping had no significant impact on the optoelectronic properties of the CQDs due to the isovalent character and similar size of the dopant with the host structure's cation[53]. In a latter paper, the interstitial location of Cu^{+} in InAs CQDs was further confirmed from XAFS measurements and DFT calculations[115]. It was further shown that at very high doping densities it is possible that Cu impurities occupy positions in neighboring unit cells and interact[115].

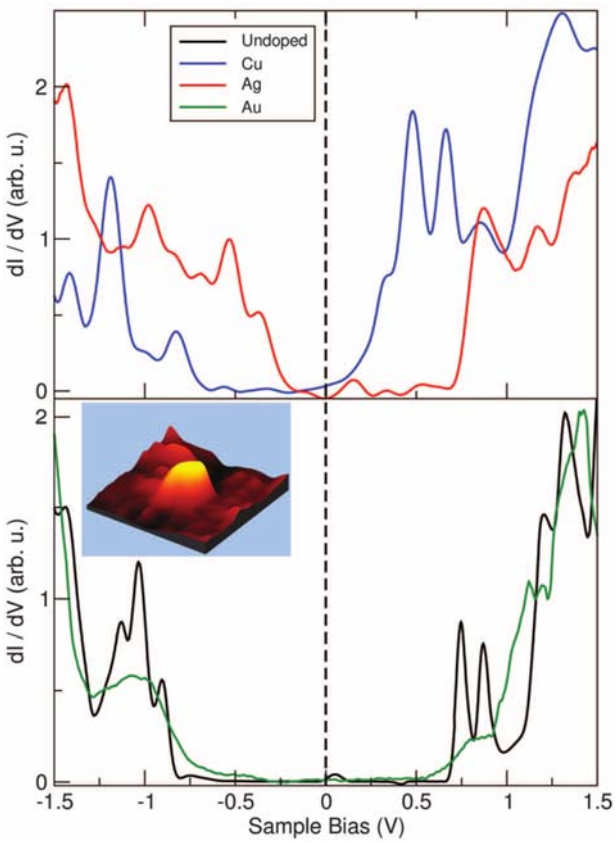

Figure 4. STM spectra of single InAs dots showing that compared to the un-doped case, Cu-doping shifts the Fermi level E_F (dashed line) close to the conduction band (n-doping), Ag doping shifts E_F close to valence band (p-doping), and Au doping has no apparent effect. Inset shows an STM image of a single dot. Adapted with permission from ref [53], Copyright 2011 The American Association for the Advancement of Science.

Another CQD material family of significant technological interest is that of lead chalcogenides and a few works report doping with aliovalent cations like Ag^{+} [19,117] and Bi^{3+} [21,118] which when substituting Pb^{2+} should in principle result to p- and n-type doping respectively. Indeed, Kang et al reported that doping, post-synthetically, PbSe CQDs with Ag^{1+} enhances the dots' p-type character as studied via electrical characterization of CQD FET structures[117]. No significant change of the electron mobility values of the films upon doping was observed[117]. In another work, Liu et al. [19] reported the optimization of p-n PbS CQD homojunctions solar cells by increasing hole density (to values up to $10^{19}cm^{-3}$) on the p-side of the junctions via post-synthetic doping of the CQDs with Ag^{+} [19]. The development of PbS CQD homojunction solar cells was also a major motivation for our recently reported work on doping the CQDs with Bi^{3+} [21]. We investigated the electrical properties of the CQDs using a variety of material characterization techniques like XPS, UPS, cyclic voltammetry, optical absorption and PL

spectroscopy, TEM as well as analysis of capacitance voltage and current-voltage electrical characteristics of Schottky junctions and p-n homojunctions[21]. We found that Bi^{3+} cations introduced during the crystallization of the CQDs, incorporate efficiently in the dots' structure and act as electron donors that raise the E_F of the material while also introducing mid-gap trap states close to the conduction band as shown in Figure 5a [21]. Doping with bismuth allowed the formation of stable n-type PbS CQD films and the development of the first QD homojunction solar cells operated in ambient conditions (Figure 5c). These solar cells exhibited J-V characteristics the polarity of which is determined by the order of the p- and n-layer of the junctions as shown in Figure 5d [21]. Finally we reported that the type and density of majority carriers of the CQD films as well as their ability to form Schottky or Ohmic junctions with various contacts are controlled by the dopant amount used as shown in Figure 5b [21].

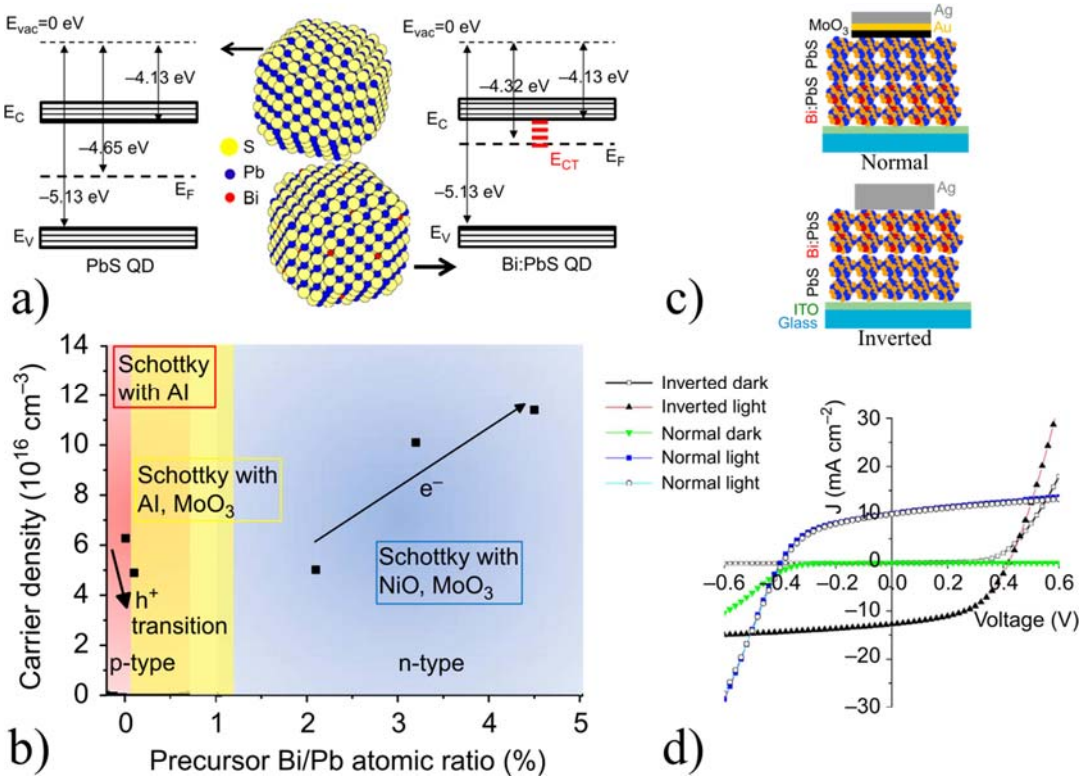

Figure 5. Schematic illustration of n-doping (shift of E_F) achieved for PbS CQDs doped with Bi^{3+}. Red lines represent dopant induced trap states (E_{CT}). b) Graph showing progressive shift from p- to n-doping of the PbS CQDs and related change of majority carrier concentrations as a function of Bi-doping. Carrier concentrations are extracted by Mott-Schottky analysis of capacitance-voltage measurements from Schottky junctions. The transformation of the doping character of the dots is also manifested by the ability to make Schottky-junctions with different electrodes. C) Schematic showing normal and inverted homojunction architectures which d) show similar photovoltaic activity under solar illumination but exhibit inverted polarity.

Adapted with permission from ref. [21] Macmillan Publishers Ltd.: Nature Communications, Copyright 2013.

3.5 Remote doping

Remote doping is a very attractive approach towards charging CQDs since it does not suffer from many of the drawbacks associated with aliovalent doping like the distortion of the crystal and electronic structure upon dopant incorporation. In the remote doping scheme, charges are injected in the dots from a material located at the close vicinity of the dots like a molecule or nanocrystal attached to the surface of the dots or from an electrode or electrolyte inside an electrochemical cell. The use of an electrochemical cell for studying the novel optical properties such as intra-band optical transitions in the IR, bleaching of the inter-band visible excitations and of the band-edge photoluminescence arising upon heavy charging of CQDs is well described in a series of works reported by Guyot-Sionnest et al for cadmium, lead and mercury chalcogenide CQDs [119–122]. Such electrochemical studies have also revealed that charging of CQD solids with electrons feeling their conduction band edge may result to increased conductivity of the films[120] as well as quick corrosion of the dots due to consumption of the extra electrons in electrochemical reactions taking place at the surface of the dots[58].

The use of an electrochemical cell for charging CQDs has provided a valuable method for investigating the various implications of charging CQDs, however is not practical for utilizing the effects of doping in optoelectronic applications. Towards that prospect, remote doping by charge donating molecules attached to the surface of the dots is a more promising approach. A number of works demonstrate heavy doping of CQDs using this approach like n-doping of CdSe by sodium biphenyl reagent[58], n-doping of PbS and PbSe by cobaltocene[123] and p-doping of PbSe CQDs by a decamethylferrocene/ decamrthylferrocenium redox buffer[59] with the last two works showing application of the thus doped CQDs films in FET devices .

In a specific example Koh et al. described heavy electronic doping of PbS and PbSe CQDs by ground state charge transfer of electrons from the cobaltocene to the conduction band of the CQDs as described in Figures 6a and 6b [123]. The occurrence, extend and driving force of the charge transfer could be controlled by both the amount of cobaltocene as well as the size of the CQDs which sets the conduction band edge offset relative to the ground state position of the cobaltocene as described in Figure 6a [123]. In an ensemble of CQDs a direct indicator of the average number of electrons transferred to the 1Se state of the dots was the extend of the bleach

of the dots' 1Sh-1Se optical absorption peak upon the introduction of the cobaltocene as seen in Figure 6c; complete bleaching of the peak indicated filling of the 1Se state of the CQDs with 8 electrons[123]. In the same report, it was further described that heavy charging of films of CQDs resulted to a large increase of their conductivity even when the CQDs were capped with oleic acid[123]. That indicated that in heavily doped PbS and PbSe CQD films conductivity is achieved by hoping through band-edge states instead of localized trap states[123]. Furthermore a clear n-type character was demonstrated when the CQD films were sequentially treated with hydrazine and cobaltocene and such films were utilized in FETs and also in p-n NiO PbSe-cobaltocene diode devices[123].

Remote doping of CQDs can also be achieved by charge transfer from another nanocrystalline phase mixed with the dots in a film. A clear demonstration of this concept was reported by Urban et al. who studied the electrical properties of Ag_2Te/PbTe nanocrystal super-lattices for application in thermoelectrics[61]. The researchers reported that the conductance of the composite films was increased by 100 times over the conductance of either of the constituent materials due to p-type doping of the PbTe by the Ag_2Te crystal phase. A similar doping concept has been proposed by us in the context of explaining the superior electrical characteristics of solar cells employing bulk nanoheterojunction (BNH) layers of PbS CQDs mixed with ZnO or Bi_2S_3 nanoparticles[60,124]. We proposed that in the mixed layers, the mid-gap trap states of the p-type PbS CQDs are partly filled with electrons donated by the nearby n-type ZnO or Bi_2S_3. This model can further explain the increase of the PbS CQDs' band-edge PL when the dots are mixed with ZnO nanoparticles[60]. Overall, remote doping of CQDs by other molecules or nanocrystalline materials is a very interesting concept however there are certain factors limiting its use in optoelectronic devices. These are related to the physical properties of the dopant material which may affect the optoelectronic properties of the overall CQDs/dopant composite in ways that are not related to the doping effect. For example, in such a solid composite, charge conductivity may take place also via the dopants and not just via the CQDs. In addition, the dopants´ optical properties will affect the overall optical properties of the composite.

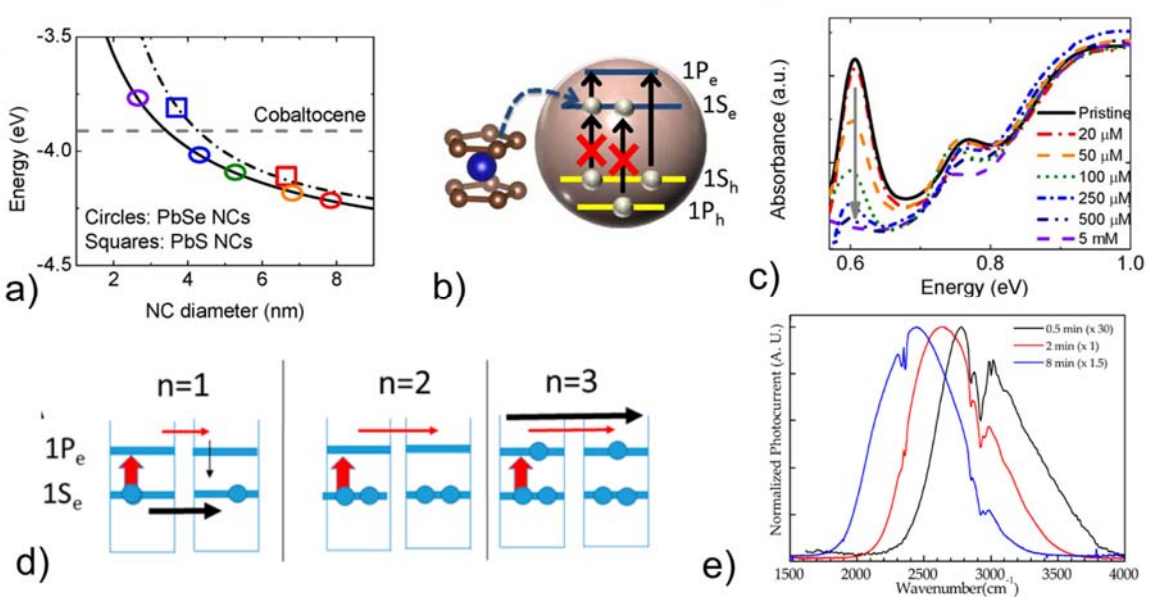

Figure 6. a) Energetic alignment of redox potential of cobaltocene in respect to the conduction band states of PbS and PbSe CQDs. d) illustration of remote electron charging of the 1Se states of the CQDs by nearby cobaltocene molecules. C) Experimentally observed progressive bleaching of the optical absorption by the first two interband transitions of PbSe CQDs with increasing cobaltocene concentration treatment. C) Diagram describing that the dark current (black arrow) and photocurrent (red arrow) in a heavily n-type HgX (X=S, Se, Te) CQD photodetector relying on intraband conduction will depend on the number n of electrons at the 1Se state. The dark current is minimized for n=2. e) Experimental demonstration of intraband photoresponce (photocurrent) using n-type HgSe CQDs the spectral response of which shifts the reaction time for the growth of the CQDs. Figures a, b, c adapted by permission from ref [123] Macmillan Publishers Ltd.: Scientific Reports, Copyright 2013. Figures d, e adapted by permission from ref [12] Copyright 2014 American Chemical Society).

4. Conclusions

Significant progress has been made towards controlling the electronic properties of CQDs for optoelectronic applications. A variety of CQD materials and doping methods have been thus far described in the literature with many demonstrating a significant degree of control of the electronic properties of CQDs films. While heavy charging of CQDs is known to trigger the appearance of uncommon optoelectronic effects potentially very useful in novel applications like mid-IR photodetectors, these effects are elusive in the majority of published reports. This is not surprising considering the existence of many fundamental challenges associated with charging the CQDs and doing so for prolonged periods of time. Achieving both of these tasks most definitely requires parallel actions towards multi-parameter material engineering.

Despite the above, for some very important applications like photovoltaics and FETs the progress made in electronic doping of CQDs has already translated to improved device performance and creation of novel device architectures like CQD quantum (homo) junctions. At the same time, recent progress made towards not only achieving heavy n-doping of mercury chalcogenide quantum dots, but also in precisely controlling the number of excess electrons to being exactly 2, as shown in Figures 6d, has allowed for the fabrication of the first CQD based photodetectors with photoresponce in the mid-IR as shown in figure 6e, exploiting intra-band photo-excitations instead of the more conventional inter-band ones[12]. The undertaken efforts on precise electronic control of CQDs do not only signify the matureness of CQDs as candidate materials for conventional optoelectronics, but also their transcendence into enablers of novel applications. Therefore, the future development of CQD based optoelectronics will depend on further advancing doping strategies which provide p- and n- doping of CQDs that is robust under various environmental conditions, permanent in time, and compatible with incorporating the dots in devices. An ultimate goal is to eventually be able to make colloidal quantum dot solutions and films for which we have the ability to select not only the size of the dots but also the type and number of free charge carriers each dot contains.

Bibliography

1. Nanocrystals in their prime. *Nat Nano* **9,** 325 (2014).

2. Alivisatos, A. P. Perspectives on the Physical Chemistry of Semiconductor Nanocrystals. *J. Phys. Chem.* **100,** 13226–13239 (1996).

3. Yuan, M., Voznyy, O., Zhitomirsky, D., Kanjanaboos, P. & Sargent, E. H. Synergistic doping of fullerene electron transport layer and colloidal quantum dot solids enhances solar cell performance. *Adv. Mater.* **27,** 917–21 (2015).

4. Labelle, A. J. *et al.* Colloidal Quantum Dot Solar Cells Exploiting Hierarchical Structuring. *Nano Lett.* **15,** 1101–1108 (2015).

5. Konstantatos, G. *et al.* Hybrid graphene-quantum dot phototransistors with ultrahigh gain. *Nat Nano* **7,** 363–368 (2012).

6. Konstantatos, G. *et al.* Ultrasensitive solution-cast quantum dot photodetectors. *Nature* **442,** 180–183 (2006).

7. Yang, Y. *et al.* High-efficiency light-emitting devices based on quantum dots with tailored nanostructures. *Nat Phot.* **9,** 259–266 (2015).

8. Shirasaki, Y., Supran, G. J., Bawendi, M. G. & Bulovic, V. Emergence of colloidal quantum-dot light-emitting technologies. *Nat Phot.* **7,** 13–23 (2013).

9. Huynh, W. U., Dittmer, J. J. & Alivisatos, A. P. Hybrid Nanorod-Polymer Solar Cells. *Sci.* **295 ,** 2425–2427 (2002).

10. McDonald, S. A. *et al.* Solution-processed PbS quantum dot infrared photodetectors and photovoltaics. *Nat Mater* **4,** 138–142 (2005).

11. Choi, M. K. *et al.* Wearable red-green-blue quantum dot light-emitting diode array using high-resolution intaglio transfer printing. *Nat Commun* **6,** (2015).

12. Deng, Z., Jeong, K. S. & Guyot-Sionnest, P. Colloidal Quantum Dots Intraband Photodetectors. *ACS Nano* **8,** 11707–11714 (2014).

13. Levine, B. F., Choi, K. K., Bethea, C. G., Walker, J. & Malik, R. J. New 10 μm infrared detector using intersubband absorption in resonant tunneling GaAlAs superlattices. *Appl. Phys. Lett.* **50,** 1092 (1987).

14. Faist, J. *et al.* Quantum Cascade Laser. *Sci.* **264 ,** 553–556 (1994).

15. Wang, C., Wehrenberg, B. L., Woo, C. Y. & Guyot-Sionnest, P. Light Emission and Amplification in Charged CdSe Quantum Dots. *J. Phys. Chem. B* **108,** 9027–9031

16. Norris, D. J., Efros, A. L. & Erwin, S. C. Doped Nanocrystals. *Sci.* **319 ,** 1776–1779 (2008).

17. Engel, J. H. & Alivisatos, A. P. Postsynthetic Doping Control of Nanocrystal Thin Films: Balancing Space Charge to Improve Photovoltaic Efficiency. *Chem. Mater.* **26,** 153–162 (2014).

18. Kramer, I. J. & Sargent, E. H. Colloidal Quantum Dot Photovoltaics: A Path Forward. *ACS Nano* **5,** 8506–8514 (2011).

19. Liu, H. *et al.* Systematic optimization of quantum junction colloidal quantum dot solar cells. *Appl. Phys. Lett.* **101,** (2012).

20. Tang, J. *et al.* Quantum junction solar cells. *Nano Lett.* **12,** 4889–4894 (2012).

21. Stavrinadis, A. *et al.* Heterovalent cation substitutional doping for quantum dot homojunction solar cells. *Nat. Commun.* **4,** 2981 (2013).

22. Hetsch, F., Zhao, N., Kershaw, S. V & Rogach, A. L. Quantum dot field effect transistors. *Mater. Today* **16,** 312–325 (2013).

23. Zhitomirsky, D. *et al.* Engineering colloidal quantum dot solids within and beyond the mobility-invariant regime. *Nat Commun* **5,** (2014).

24. Nagpal, P. & Klimov, V. I. Role of mid-gap states in charge transport and photoconductivity in semiconductor nanocrystal films. *Nat Commun* **2,** 486 (2011).

25. Milliron, D. J. Quantum dot solar cells: The surface plays a core role. *Nat Mater* **13,** 772–773 (2014).

26. Tang, J. *et al.* Colloidal-quantum-dot photovoltaics using atomic-ligand passivation. *Nat Mater* **10,** 765–771 (2011).

27. Gai, Y., Peng, H. & Li, J. Electronic Properties of Nonstoichiometric PbSe Quantum Dots from First Principles. *J. Phys. Chem. C* **113,** 21506–21511 (2009).

28. Kim, D., Kim, D. H., Lee, J. H. & Grossman, J. C. Impact of stoichiometry on the electronic structure of PbS quantum dots. *Phys. Rev. Lett.* **110,** 1–5 (2013).

29. Voznyy, O. Mobile Surface Traps in CdSe Nanocrystals with Carboxylic Acid Ligands. *J. Phys. Chem. C* **115,** 15927–15932 (2011).

30. Yin, Y. & Alivisatos, A. P. Colloidal nanocrystal synthesis and the organic-inorganic interface. *Nature* **437,** 664–670 (2005).

31. Ihly, R., Tolentino, J., Liu, Y., Gibbs, M. & Law, M. The Photothermal Stability of PbS Quantum Dot Solids. *ACS Nano* **5,** 8175–8186 (2011).

32. Tang, J. *et al.* Quantum Dot Photovoltaics in the Extreme Quantum Confinement Regime: The Surface-Chemical Origins of Exceptional Air- and Light-Stability. *ACS Nano* **4,** 869–878 (2010).

33. Zherebetskyy, D. *et al.* Hydroxylation of the surface of PbS nanocrystals passivated with oleic acid. *Sci.* **344 ,** 1380–1384 (2014).

34. Voznyy, O. *et al.* A Charge-Orbital Balance Picture of Doping in Colloidal Quantum Dot Solids. *ACS Nano* **6,** 8448–8455 (2012).

35. Talapin, D. V & Murray, C. B. PbSe Nanocrystal Solids for n- and p-Channel Thin Film Field-Effect Transistors. *Sci.* **310 ,** 86–89 (2005).

36. Oh, S. J. *et al.* Stoichiometric Control of Lead Chalcogenide Nanocrystal Solids to Enhance Their Electronic and Optoelectronic Device Performance. *ACS Nano* **7,** 2413–2421 (2013).

37. Luther, J. M. & Pietryga, J. M. Stoichiometry control in quantum dots: A viable analog to impurity doping of bulk materials. *ACS Nano* **7,** 1845–1849 (2013).

38. Voznyy, O., Thon, S. M., Ip, A. H. & Sargent, E. H. Dynamic trap formation and elimination in colloidal quantum dots. *J. Phys. Chem. Lett.* **4,** 987–992 (2013).

39. Anderson, N. C. & Owen, J. S. Soluble, Chloride-Terminated CdSe Nanocrystals: Ligand Exchange Monitored by 1H and 31P NMR Spectroscopy. *Chem. Mater.* **25,** 69–76 (2013).

40. Dai, Q. *et al.* Size-Dependent Composition and Molar Extinction Coefficient of PbSe Semiconductor Nanocrystals. *ACS Nano* **3,** 1518–1524 (2009).

41. Moreels, I. *et al.* Composition and Size-Dependent Extinction Coefficient of Colloidal PbSe Quantum Dots. *Chem. Mater.* **19,** 6101–6106 (2007).

42. Morris-Cohen, A. J., Frederick, M. T., Lilly, G. D., McArthur, E. A. & Weiss, E. A. Organic Surfactant-Controlled Composition of the Surfaces of CdSe Quantum Dots. *J. Phys. Chem. Lett.* **1,** 1078–1081 (2010).

43. Smith, D. K., Luther, J. M., Semonin, O. E., Nozik, A. J. & Beard, M. C. Tuning the Synthesis of Ternary Lead Chalcogenide Quantum Dots by Balancing Precursor Reactivity. *ACS Nano* **5,** 183–190 (2011).

44. Moreels, I., Fritzinger, B., Martins, J. C. & Hens, Z. Surface Chemistry of Colloidal PbSe Nanocrystals. *J. Am. Chem. Soc.* **130,** 15081–15086 (2008).

45. Bekenstein, Y. *et al.* Thermal Doping by Vacancy Formation in Copper Sulfide Nanocrystal Arrays. *Nano Lett.* **14,** 1349–1353 (2014).

46. Luther, J. M., Jain, P. K., Ewers, T. & Alivisatos, A. P. Localized surface plasmon resonances arising from free carriers in doped quantum dots. *Nat Mater* **10,** 361–366 (2011).

47. Scotognella, F. *et al.* Plasmon Dynamics in Colloidal Cu2–xSe Nanocrystals. *Nano Lett.* **11,** 4711–4717 (2011).

48. Tang, J. *et al.* Heavy-metal-free solution-processed nanoparticle-based photodetectors: Doping of intrinsic vacancies enables engineering of sensitivity and speed. *ACS Nano* **3,** 331–338 (2009).

49. Turnbull, D. Formation of Crystal Nuclei in Liquid Metals. *J. Appl. Phys.* **21,** 1022 (1950).

50. Dalpian, G. M. & Chelikowsky, J. R. Self-Purification in Semiconductor Nanocrystals. *Phys. Rev. Lett.* **96,** 226802 (2006).

51. Chan, T.-L., Tiago, M. L., Kaxiras, E. & Chelikowsky, J. R. Size Limits on Doping Phosphorus into Silicon Nanocrystals. *Nano Lett.* **8,** 596–600 (2008).

52. Chikan, V. Challenges and Prospects of Electronic Doping of Colloidal Quantum Dots: Case Study of CdSe. *J. Phys. Chem. Lett.* **2,** 2783–2789 (2011).

53. Mocatta, D. *et al.* Heavily Doped Semiconductor Nanocrystal Quantum Dots. *Sci.* **332 ,** 77–81 (2011).

54. Bryan, J. D. & Gamelin, D. R. in *Progress in Inorganic Chemistry* 47–126 (John Wiley & Sons, Inc., 2005). doi:10.1002/0471725560.ch2

55. Holmberg, V. C., Helps, J. R., Mkhoyan, K. A. & Norris, D. J. Imaging Impurities in Semiconductor Nanostructures. *Chem. Mater.* **25,** 1332–1350 (2013).

56. Yang, Y., Chen, O., Angerhofer, A. & Cao, Y. C. Radial-Position-Controlled Doping in CdS/ZnS Core/Shell Nanocrystals. *J. Am. Chem. Soc.* **128,** 12428–12429 (2006).

57. Koh, W. *et al.* Heavily doped n-type PbSe and PbS nanocrystals using ground-state charge transfer from cobaltocene. *Sci. Rep.* **3,** (2013).

58. Shim, M. & Guyot-Sionnest, P. n-type colloidal semiconductor nanocrystals. *Nature* **407,** 981–983 (2000).

59. Engel, J. H., Surendranath, Y. & Alivisatos, A. P. Controlled Chemical Doping of Semiconductor Nanocrystals Using Redox Buffers. *J. Am. Chem. Soc.* **134,** 13200–13203 (2012).

60. Rath, A. K. *et al.* Remote trap passivation in colloidal quantum dot bulk nano-heterojunctions and its effect in solution-processed solar cells. *Adv. Mater.* **26,** 4741–4747 (2014).

61. Urban, J. J., Talapin, D. V, Shevchenko, E. V, Kagan, C. R. & Murray, C. B. Synergism in binary nanocrystal superlattices leads to enhanced p-type conductivity in self-assembled PbTe/Ag2Te thin films. *Nat Mater* **6,** 115–121 (2007).

62. Wang, C., Shim, M. & Guyot-Sionnest, P. Electrochromic Nanocrystal Quantum Dots. *Sci.* **291 ,** 2390–2392 (2001).

63. Wehrenberg, B. L. & Guyot-Sionnest, P. Electron and Hole Injection in PbSe Quantum Dot Films. *J. Am. Chem. Soc.* **125,** 7806–7807 (2003).

64. Luo, H. *et al.* Synthesis and Characterization of Gallium-Doped CdSe Quantum Dots. *J. Phys. Chem. C* **119,** 10749–10757 (2015).

65. Koleilat, G. I. *et al.* Efficient, Stable Infrared Photovoltaics Based on Solution-Cast Colloidal Quantum Dots. *ACS Nano* **2,** 833–840 (2008).

66. Luther, J. M. *et al.* Structural, Optical, and Electrical Properties of Self-Assembled Films of PbSe Nanocrystals Treated with 1,2-Ethanedithiol. *ACS Nano* **2,** 271–280 (2008).

67. Konstantatos, G., Levina, L., Fischer, A. & Sargent, E. H. Engineering the Temporal Response of Photoconductive Photodetectors via Selective Introduction of Surface Trap States. *Nano Lett.* **8,** 1446–1450 (2008).

68. Leschkies, K. S., Kang, M. S., Aydil, E. S. & Norris, D. J. Influence of Atmospheric Gases on the Electrical Properties of PbSe Quantum-Dot Films. *J. Phys. Chem. C* **114,** 9988–9996 (2010).

69. Brown, P. R. *et al.* Energy Level Modification in Lead Sulfide Quantum Dot Thin Films through Ligand Exchange. *ACS Nano* **8,** 5863–5872 (2014).

70. Gao, J. *et al.* Quantum Dot Size Dependent J−V Characteristics in Heterojunction ZnO/PbS Quantum Dot Solar Cells. *Nano Lett.* **11,** 1002–1008 (2011).

71. Yoon, W. *et al.* Enhanced open-circuit voltage of PbS nanocrystal quantum dot solar cells. *Sci. Rep.* **3,** 2225 (2013).

72. Barkhouse, D. A. R., Pattantyus-Abraham, A. G., Levina, L. & Sargent, E. H. Thiols Passivate Recombination Centers in Colloidal Quantum Dots Leading to Enhanced Photovoltaic Device Efficiency. *ACS Nano* **2,** 2356–2362 (2008).

73. Luther, J. M. *et al.* Schottky Solar Cells Based on Colloidal Nanocrystal Films. *Nano Lett.* **8,** 3488–3492 (2008).

74. Jeong, K. S. *et al.* Enhanced Mobility-Lifetime Products in PbS Colloidal Quantum Dot Photovoltaics. *ACS Nano* **6,** 89–99 (2012).

75. Hwang, G. W. *et al.* Identifying and Eliminating Emissive Sub-bandgap States in Thin Films of PbS Nanocrystals. *Adv. Mater.* (2015). doi:10.1002/adma.201501156

76. Carey, G. H. *et al.* Electronically Active Impurities in Colloidal Quantum Dot Solids. *ACS Nano* **8,** 11763–11769 (2014).

77. Ning, Z. *et al.* Air-stable n-type colloidal quantum dot solids. *Nat. Mater.* **13,** 4–10 (2014).

78. Ning, Z. *et al.* All-inorganic colloidal quantum dot photovoltaics employing solution-phase halide passivation. *Adv. Mater.* **24,** 6295–6299 (2012).

79. Ip, A. H. *et al.* Hybrid passivated colloidal quantum dot solids. *Nature Nanotechnology* **7,** 577–582 (2012).

80. Zhitomirsky, D. *et al.* N-type colloidal-quantum-dot solids for photovoltaics. *Adv. Mater.* **24,** 6181–5 (2012).

81. Yuan, M. *et al.* Doping Control Via Molecularly Engineered Surface Ligand Coordination. *Adv. Mater.* **25,** 5586–5592 (2013).

82. Fafarman, A. T. *et al.* Thiocyanate-Capped Nanocrystal Colloids: Vibrational Reporter of Surface Chemistry and Solution-Based Route to Enhanced Coupling in Nanocrystal Solids. *J. Am. Chem. Soc.* **133,** 15753–15761 (2011).

83. Kovalenko, M. V, Scheele, M. & Talapin, D. V. Colloidal Nanocrystals with Molecular Metal Chalcogenide Surface Ligands. *Sci.* **324 ,** 1417–1420 (2009).

84. Nag, A. *et al.* Effect of Metal Ions on Photoluminescence, Charge Transport, Magnetic and Catalytic Properties of All-Inorganic Colloidal Nanocrystals and Nanocrystal Solids. *J. Am. Chem. Soc.* **134,** 13604–13615 (2012).

85. Dos Santos, A. P. & Levin, Y. Ion Specificity and the Theory of Stability of Colloidal Suspensions. *Phys. Rev. Lett.* **106,** 167801 (2011).

86. Grosberg, A. Y., Nguyen, T. T. & Shklovskii, B. I. \textit{Colloquium} : The physics of charge inversion in chemical and biological systems. *Rev. Mod. Phys.* **74,** 329–345 (2002).

87. Li, H.-Y. *et al.* Remote p-Doping of InAs Nanowires. *Nano Lett.* **7,** 1144–1148 (2007).

88. Crisp, R. W. *et al.* Metal Halide Solid-State Surface Treatment for High Efficiency PbS and PbSe QD Solar Cells. *Sci. Rep.* **5,** (2015).

89. Chuang, C.-H. M., Brown, P. R., Bulović, V. & Bawendi, M. G. Improved performance and stability in quantum dot solar cells through band alignment engineering. *Nat. Mater.* **13,** 1–6 (2014).

90. Jeong, K. S., Deng, Z., Keuleyan, S., Liu, H. & Guyot-Sionnest, P. Air-Stable n-Doped Colloidal HgS Quantum Dots. *J. Phys. Chem. Lett.* **5,** 1139–1143 (2014).

91. Bekenstein, Y. *et al.* Thermal Doping by Vacancy Formation in Copper Sulfide Nanocrystal Arrays. *Nano Lett.* **14,** 1349–1353 (2014).

92. Son, D. H., Hughes, S. M., Yin, Y. & Paul Alivisatos, A. Cation Exchange Reactions in Ionic Nanocrystals. *Sci.* **306 ,** 1009–1012 (2004).

93. Rivest, J. B. & Jain, P. K. Cation exchange on the nanoscale: an emerging technique for new material synthesis, device fabrication, and chemical sensing. *Chem. Soc. Rev.* **42,** 89–96 (2013).

94. Stowell, C. A., Wiacek, R. J., Saunders, A. E. & Korgel, B. A. Synthesis and Characterization of Dilute Magnetic Semiconductor Manganese-Doped Indium Arsenide Nanocrystals. *Nano Lett.* **3,** 1441–1447 (2003).

95. Viswanatha, R., Brovelli, S., Pandey, A., Crooker, S. A. & Klimov, V. I. Copper-Doped Inverted Core/Shell Nanocrystals with 'Permanent' Optically Active Holes. *Nano Lett.* **11,** 4753–4758 (2011).

96. Xie, R. & Peng, X. Synthesis of Cu-Doped InP Nanocrystals (d-dots) with ZnSe Diffusion Barrier as Efficient and Color-Tunable NIR Emitters. *J. Am. Chem. Soc.* **131,** 10645–10651 (2009).

97. Orlinskii, S. B. *et al.* Probing the Wave Function of Shallow Li and Na Donors in ZnO Nanoparticles. *Phys. Rev. Lett.* **92,** 47603 (2004).

98. Pi, X. D., Gresback, R., Liptak, R. W., Campbell, S. A. & Kortshagen, U. Doping efficiency, dopant location, and oxidation of Si nanocrystals. *Appl. Phys. Lett.* **92,** 123102 (2008).

99. Stegner, A. R. *et al.* Electronic Transport in Phosphorus-Doped Silicon Nanocrystal Networks. *Phys. Rev. Lett.* **100,** 26803 (2008).

100. Fujii, M., Yamaguchi, Y., Takase, Y., Ninomiya, K. & Hayashi, S. Photoluminescence from impurity codoped and compensated Si nanocrystals. *Appl. Phys. Lett.* **87,** 211919 (2005).

101. Gresback, R. *et al.* Controlled Doping of Silicon Nanocrystals Investigated by Solution-Processed Field Effect Transistors. *ACS Nano* **8,** 5650–5656 (2014).

102. Wills, A. W. *et al.* Synthesis and characterization of Al- and In-doped CdSe nanocrystals. *J. Mater. Chem.* **22,** 6335–6342 (2012).

103. Choi, J.-H. *et al.* Bandlike Transport in Strongly Coupled and Doped Quantum Dot Solids: A Route to High-Performance Thin-Film Electronics. *Nano Lett.* **12,** 2631–2638 (2012).

104. Tuinenga, C., Jasinski, J., Iwamoto, T. & Chikan, V. In Situ Observation of Heterogeneous Growth of CdSe Quantum Dots: Effect of Indium Doping on the Growth Kinetics. *ACS Nano* **2,** 1411–1421 (2008).

105. Knox, C. K. *et al.* Synthesis and characterization of photoluminescent In-doped CdSe nanoparticles. *J. Colloid Interface Sci.* **300,** 591–596 (2006).

106. Roy, S. *et al.* Progress toward producing n-type CdSe quantum dots: Tin and indium doped CdSe quantum dots. *J. Phys. Chem. C* **113,** 13008–13015 (2009).

107. Sahu, A. *et al.* Electronic Impurity Doping in CdSe Nanocrystals. *Nano Lett.* **12,** 2587–2594 (2012).

108. Ott, F. D., Spiegel, L. L., Norris, D. J. & Erwin, S. C. Microscopic Theory of Cation Exchange in CdSe Nanocrystals. *Phys. Rev. Lett.* **113,** 156803 (2014).

109. Meulenberg, R. W. *et al.* Structure and composition of Cu-doped CdSe nanocrystals using soft X-ray absorption spectroscopy. *Nano Lett.* **4,** 2277–2285 (2004).

110. Wang, X. *et al.* Non-blinking semiconductor nanocrystals. *Nature* **459,** 686–689 (2009).

111. Spinicelli, P. *et al.* Bright and Grey States in CdSe-CdS Nanocrystals Exhibiting Strongly Reduced Blinking. *Phys. Rev. Lett.* **102,** 136801 (2009).

112. Klimov, V. I. *et al.* Optical Gain and Stimulated Emission in Nanocrystal Quantum Dots. *Sci.* **290 ,** 314–317 (2000).

113. Kompch, A. *et al.* Localization of Ag Dopant Atoms in CdSe Nanocrystals by Reverse Monte Carlo Analysis of EXAFS Spectra. *J. Phys. Chem. C* (2015). doi:10.1021/acs.jpcc.5b04399

114. Geyer, S. M. *et al.* Control of the Carrier Type in InAs Nanocrystal Films by Predeposition Incorporation of Cd. *ACS Nano* **4,** 7373–7378 (2010).

115. Amit, Y. *et al.* Unraveling the Impurity Location and Binding in Heavily Doped Semiconductor Nanocrystals: The Case of Cu in InAs Nanocrystals. *J. Phys. Chem. C* **117,** 13688–13696 (2013).

116. Hang, Q. *et al.* Role of Molecular Surface Passivation in Electrical Transport Properties of InAs Nanowires. *Nano Lett.* **8,** 49–55 (2008).

117. Kang, M. S., Sahu, A., Frisbie, C. D. & Norris, D. J. Influence of silver doping on electron transport in thin films of PbSe nanocrystals. *Adv. Mater.* **25,** 725–31 (2013).

118. Saha, S. K., Bera, A. & Pal, A. J. Improvement in PbS-based Hybrid Bulk-Heterojunction Solar Cells through Band Alignment via Bismuth Doping in the Nanocrystals. *ACS Appl. Mater. Interfaces* **7,** 8886–8893 (2015).

119. Wang, C. Electrochromic Nanocrystal Quantum Dots. *Science (80-.).* **291,** 2390–2392 (2001).

120. Yu, D., Wang, C. & Guyot-Sionnest, P. n-Type Conducting CdSe Nanocrystal Solids. *Sci.* **300 ,** 1277–1280 (2003).

121. Wehrenberg, B. L. & Guyot-Sionnest, P. Electron and Hole Injection in PbSe Quantum Dot Films. *J. Am. Chem. Soc.* **125,** 7806–7807 (2003).

122. Liu, H., Keuleyan, S. & Guyot-Sionnest, P. n- and p-Type HgTe Quantum Dot Films. *J. Phys. Chem. C* **116,** 1344–1349 (2012).

123. Koh, W. *et al.* Heavily doped n-type PbSe and PbS nanocrystals using ground-state charge transfer from cobaltocene. *Sci. Rep.* **3,** (2013).

124. Rath, A. K. *et al.* Solution-processed inorganic bulk nano-heterojunctions and their application to solar cells. *Nat Phot.* **6,** 529–534 (2012).